Purification of Single-Wall Carbon Nanotubes by Electrochemical Oxidation

Hai-Tao Fang,[†,‡] Chen-Guang Liu,[†] Chang Liu,[†] Feng Li,[†] Min Liu,[†] and Hui-Ming Cheng*[,†]

Shenyang National Laboratory for Materials Science, Institute of Metal Research, Chinese Academy of Sciences, 72 Wenhua Road, Shenyang 110016, China, and Materials Science and Engineering School, Harbin Institute of Technology, 92 West Dazhi Street, Harbin 150001, China

Received December 3, 2003. Revised Manuscript Received August 22, 2004

The electrochemical cyclic voltammetric (CV) oxidation behavior of an arc-derived single-wall carbon nanotube (SWNT) sample in potassium hydroxide solution was investigated. Amorphous carbon in the as-grown SWNT sample was effectively removed by the CV oxidation, as confirmed by analyzing the sp^3/sp^2 carbon ratio from C1s XPS spectra and HRTEM observations. The removal of the amorphous carbon led to the exposure of metal nanoparticles, hence facilitating the elimination of the metal impurities by subsequent HCl washing. The CV oxidation can be applied as an alternative oxidative treatment for the purification of SWNT samples. Redox peaks were observed during the CV oxidation. The reduction peaks in the range of −0.96 to −1.0 V and the oxidation peaks in the range of −0.61 to −0.49 V were attributed to the electrochemical redox transformations between metallic Fe and Fe(II) oxide, Fe(II) oxide and Fe(III) oxide, as well as Ni and Ni(II) oxide, and the observed reduction peaks in the potential range of 0.29−0.13 V were believed to be caused by the electrochemical reduction of NiOOH into $Ni(OH)_2$. The intensity of all of the redox peaks was dependent on the cycle number because more and more metal nanoparticles could be exposed as a result of the incremental removal or damage of the amorphous carbon coating during the CV oxidation, while the intensity remained almost unchanged after 80 cycles because of the completion of the amorphous carbon removal. Therefore, the redox peaks from the electrochemical redox reactions of Fe and Ni impurities can be considered as a benchmark for the removal extent of the amorphous carbon, and optimal electrochemical oxidation time for the purification of the as-grown SWNT sample can be determined in real time during the CV oxidation treatment. This is a predominant advantage of the CV oxidation over common oxidation methods using air or other oxidizing reagents for SWNT purification.

Introduction

Since the discovery of single-wall carbon nanotubes (SWNTs) in 1993,[1,2] they have attracted great interest because of their novel structural, electrical, and mechanical properties. Many useful applications of SWNTs including field emission devices,[3] nanoelectronics,[4] structural composites,[5] hydrogen storage,[6] sensors,[7] actuators,[8] and electrochemical storage and production of energy[9−11] have been proposed. However, as-grown SWNT products can hardly be used directly because they often contain a certain amount of metal catalyst residue existing as nanoparticles and carbonaceous byproducts such as fullerenes, nanocrystalline graphite, and amorphous carbon usually covering nanotubes and metal nanoparticles. These impurities degrade the best performance of SWNTs in functional devices and sometimes hinder accurate analysis of the physical properties of SWNTs.[12] Therefore, the purification of SWNT products is one of the most fundamental steps before they are used for research and technological applications.

By taking advantage of the difference in oxidation rate between carbon nanotubes and carbon byproducts, oxidative treatments, such as wet oxidation and gas

* Corresponding author. Phone: 86-24-23971611. Fax: 86-24-23891320. E-mail: cheng@imr.ac.cn.
† Chinese Academy of Sciences.
‡ Harbin Institute of Technology.

(1) Iijima, S.; Ichihashi, T. *Nature* **1993**, *363*, 603.
(2) Bethune, D. S.; Kiang, C. H.; de Vries, M. S.; Gorman, G.; Savoy, R.; Vazques, J.; Beyers, R. *Nature* **1993**, *363*, 605.
(3) Baughman, R. H.; Zakhidov, A. A.; de Heer, W. A. *Science* **2002**, *297*, 787.
(4) Tans, S. J.; Verschueren, A. R. M.; Dekker, C. *Natrue* **1998**, *393*, 49.
(5) Ajayan, P. M.; Schadler, L. S.; Giannaris, C.; Rubio, A. *Adv. Mater.* **2000**, *12*, 750.
(6) Liu, C.; Fan, Y. Y.; Liu, M.; Cong, H. T.; Cheng, H. M.; Dresselhaus, M. S. *Science* **1999**, *286*, 1127.
(7) Kong, J.; Franklin, N. R.; Zhou, C. H.; Chapline, M. G.; Peng, S.; Cho, K.; Dai, H. *Science* **2000**, *287*, 622.
(8) Baughman, R. H.; Cui, C. X.; Zakhidov, A. A.; Iqbal, Z.; Barisci, J. N.; Spinks, G. M.; Wallace, G. G.; Mazzoldi, A.; De Rossi, D.; Rinzler, A. G.; Jaschinski, O.; Roth, S.; Kertesz, M. *Science* **1999**, *284*, 1340.
(9) Che, G. L.; Lakshmi, B. B.; Fisher, E. R.; Martin, C. R. *Nature* **1998**, *393*, 346.
(10) Frackowiak, E.; Béguin, F. *Carbon* **2002**, *40*, 1775.
(11) Guldi, D. M.; Marcaccio, M.; Paolucci, D.; Paolucci, F.; Tagmatarchis, N.; Tasis, D.; Vázquez, E.; Proto, M. *Angew. Chem., Int. Ed.* **2003**, *42*, 4206.
(12) Grigorian, L.; Sumanasekera, G. U.; Loper, A. L.; Fang, S. L.; Allen, J. L.; Eklund, P. C. *Phys. Rev. B* **1999**, *60*, 11309.

10.1021/cm035263h CCC: $27.50
Published on Web 11/17/2004

phase oxidation, are commonly involved in purification procedures. The wet oxidation refers to the oxidation using a solution containing strong oxidizing reagents such as HNO_3 and H_2O_2.[13−16] The gas-phase oxidation by air or oxygen is commonly used for purifying multiwall carbon nanotubes (MWNTs) and has also been developed for SWNT purification.[17−20] The treatment conditions for these two conventional oxidation methods have to be optimized, otherwise overoxidation may damage the carbon nanotubes and lead to a very low yield. However, the quality and composition of as-grown SWNT products from different synthesis methods, or even from different batches of the same synthesis method, are different. For this reason, one has to separately carry out oxidation treatments several times to seek an optimal oxidation time and intensity for each batch of SWNT products. A key point lies in the absence of a benchmark during the conventional oxidations, indicating when the removal of amorphous carbon in SWNT products is completed.

The study of the electrochemical oxidation of carbon nanotubes in aqueous electrolyte solutions for different purposes including doping, functionalization, tips opening, and purification has been described only in a few literature.[21−25] Sumanasekera and co-workers attained the doping of bisulfate ions into SWNTs by an electrochemical oxidation process in sulfuric acid.[21] Unger et al. carried out the electrochemical oxidation of MWNTs in NaCl or NaBr solution and realized the halogenation of MWNTs and the formation of oxygen-containing functional groups on MWNTs.[22] To improve electrochemical hydrogen storage in MWNTs, Skowroński et al. realized the opening of MWNTs' tips by scanning the potential above 1.15 V (vs Hg/Hg_2SO_4), at which the electrochemical oxidation of the MWNTs occurred.[23] Yang et al. presented a process for MWNT purification by a galvanostatic electrochemical oxidation in sulfuric acid, and they attributed the purification mechanism to the faster oxidation rate of amorphous carbon than that of MWNTs.[24] Ito et al. studied the etching of individual MWNT in a KCl solution by applying a positive potential higher enough for the occurrence of the electrochemical oxidation. They also found that the amorphous carbon layer was etched more readily than the MWNT core.[25]

Similar to wet oxidation and gas-phase oxidation, carbon materials with fewer defects usually show a lower corrosion rate under electrochemical oxidation. For example, the oxidation rate of graphite was considerably lower than that of amorphous carbon in alkaline solutions.[26] Therefore, it is reasonable to deduce that carbon nanotubes with fewer defects than amorphous carbon should show higher electrochemical oxidation resistance. The difference in electrochemical oxidation rate implies that the electrochemical oxidation can be used for the purification of as-grown SWNT products. To the best of our knowledge, however, no article has reported a SWNT purification method based on electrochemical oxidation. In this paper, the electrochemical cyclic voltammetric (CV) oxidation behavior of an arc-derived SWNT sample in KOH solution was investigated and the potential development of this oxidation process for SWNT purification was demonstrated. The advantages of the CV oxidation over gas oxidation and wet oxidation were illustrated.

Experimental Section

Preparation of SWNT Sample. The SWNT sample used was synthesized by the hydrogen arc-discharge method using MWNTs and carbon nanofibers (MWNTs/CNFs) with 40−300 nm diameter distribution as carbon feedstock. The fabrication process has been described in detail elsewhere.[27,28] Briefly, the electric arc was operated with 150 A direct current in a hydrogen atmosphere of 200 Torr as buffer gas. A mixture of 10 wt % Ni, 3 wt % Fe, and 3 wt % Co as metal catalysts, 4 wt % FeS as a promoter, and the MWNT/CNF powders was packed into holes on a graphite cylinder to be used as the anode. The cathode was a pure graphite rod. The MWNT/CNF powders used were prepared by the catalytic decomposition of hydrocarbons in large scale by our group.[29]

SWNT Purification by Electrochemical Cyclic Voltammetric Oxidation. Electrochemical cyclic voltammetric (CV) oxidation was conducted in a 6 M KOH electrolytic solution at room temperature and atmospheric pressure using a standard three-electrode cell. The as-grown film-like SWNT sample of about 25 mg, collected from the arc-discharge chamber wall, was sandwiched and pressed between two Pt webs to prepare a working electrode. Two Pt plates facing to the working electrode served as counter electrodes, and Hg/HgO (6 M KOH) was the reference electrode ($\varphi^0 = 0.05$ V). All potentials were measured versus the Hg/HgO reference electrode. A Solartron1287 potentiostat connecting with the three-electrode cell was used to perform CV experiments. The scan range of the CV oxidation was from −1.3 to 0.78 V, and the scan rate was 50 mV/s. After the CV oxidation was run for 80 cycles, the SWNT sample was treated in a concentrated hydrochloric acid to dissolve metal nanoparticles.

Characterization of SWNT Samples and Evaluation of the Content of Metal Impurities. High-resolution transmission electron microscopy (HRTEM) was used to observe the structure and morphology of SWNT samples. X-ray diffraction (XRD) was performed to identify the phases, especially metal nanoparticles, existing in SWNT samples. Chemical analysis of SWNT samples was performed using X-ray photoelectron

(13) Rinzler, A.; Liu, J.; Dai, H.; Nikolaev, P.; Huffman, C. B.; Rodríguez-Macías, F. L.; Boul, P. J.; Lu, A. H.; Heymann, D.; Colbert, D. T.; Lee, R. S.; Fischer, J. E.; Rao, A. M.; Eklund, P. C.; Smalley, R. E. *Appl. Phys. A* **1998**, *67*, 29.
(14) Durjardin, E.; Ebbesen, T. W.; Krishana, A.; Treacy, M. M. J. *Adv. Mater.* **1998**, *10*, 611.
(15) Zhou, O.; Gao, B.; Bower, C.; Fleming, L.; Shimoda, H. *Mol. Cryst. Liq. Cryst.* **2000**, *340*, 541.
(16) Martínez, M. T.; Callejas, M. A.; Benito, A. M.; Cochet, M.; Seeger, T.; Ansón, A.; Schreiber, J.; Gordon, C.; Marhic, C.; Chauvet, O.; Fierro, J. L. G.; Maser, W. K. *Carbon* **2003**, *41*, 2247.
(17) Shi, Z. J.; Lian, Y. F.; Liao, F. H.; Zhou, X. H.; Gu, Z. N.; Zhang, Y. G.; Iijima, S. *Solid State Commun.* **1999**, *112*, 35.
(18) Chiang, I. W.; Brinson, B. E.; Huang, A. Y.; Willis, P. A.; Bronikowaki, M. J.; Margrave, J. L.; Smalley, R. E.; Hauge, R. H. *J. Phys. Chem. B* **2001**, *105*, 8297.
(19) Moon, J. M.; An, K. H.; Lee, Y. H.; Park, Y. S.; Bae, D. J.; Park, G. S. *J. Phys. Chem. B* **2001**, *105*, 5677.
(20) Hou, P. X.; Liu, C.; Tong, Y.; Xu, S. T.; Liu, M.; Cheng, H. M. *J. Mater. Res.* **2001**, *16*, 2526.
(21) Sumanasekera, G. U.; Allen, J. L.; Fang, S. L.; Loper, A. L.; Rao, A. M.; Eklund, P. C. *J. Phys. Chem. B* **1999**, *103*, 4292.
(22) Unger, E.; Graham, A.; Kreupl, F.; Liebau, M.; Hoenlein, W. *Curr. Appl. Phys.* **2002**, *2*, 107.
(23) Skowroński, J. M.; Scharff, P.; Pfänder, N.; Cui, S. *Adv. Mater.* **2003**, *15*, 55.
(24) Yang, Z. H.; Wu, H. Q.; Li, J.; Li, X. H. *Chem. J. Chin. Univ.* **2001**, *22*, 446.
(25) Ito, T.; Sun L.; Crooks, R. M. *Electrochem. Solid-State Lett.* **2003**, *6*, C4.
(26) Kinoshita, K. *Carbon: electrochemcial and physicochemical properties*; Wiley: New York, 1987; p 334.
(27) Zhong, R.; Cong, H. T.; Liu, C. *Carbon* **2002**, *40*, 2961.
(28) Liu, C.; Cong, H. T.; Li, F.; Tan, P. H.; Cheng, H. M.; Lu, K.; Zhou, B. L. *Carbon* **1999**, *37*, 1865.
(29) Fan, Y. Y.; Li, F.; Cheng, H. M.; Su, G.; Yu, Y. D.; Shen, Z. H. *J. Mater. Res.* **1998**, *13*, 2342.

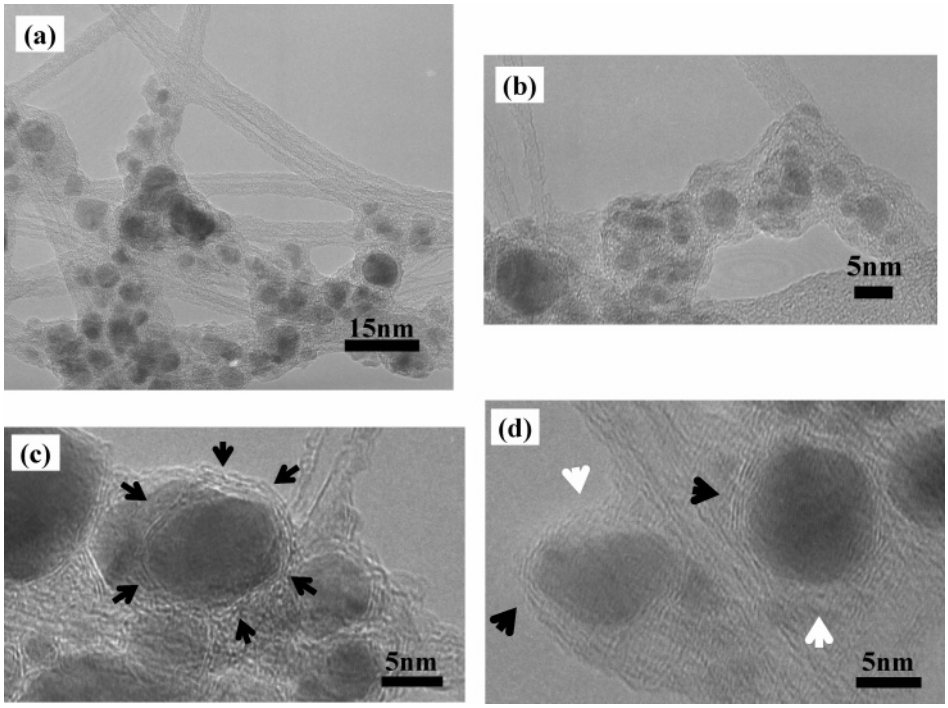

Figure 1. HRTEM micrographs of (a) the as-grown SWNT product; (b) the metal nanoparticles covered by amorphous carbon layer; (c) the metal nanoparticles covered by continuous graphitic multi-shell carbon; and (d) the metal nanoparticles covered partially by graphitic multi-shell carbon and partially by amorphous carbon.

spectroscopy (XPS). Thermogravimetric analysis (TGA) was carried out in a thermogravimetric analyzer to compare the content of metal nanoparticles in the samples before and after the purification treatment. The conditions were 10 °C/min ramp rates from room temperature to 1100 °C at an air flow rate of 20 mL/min.

Results and Discussion

As-Grown SWNT Sample. The samples used were selected from a batch of as-grown SWNT product to prove the effectiveness of this purification procedure. Figure 1 shows the HRTEM images of the as-grown SWNT product. The nanotubes and their bundles are entangled, and a significant amount of metal nanoparticles, arisen from the metal catalysts, exists in the selected as-grown SWNT sample (Figure 1a). It is obvious that amorphous carbon covers the nanotubes and their bundles. Most metal nanoparticles are encased in either amorphous carbon layer (Figure 1b) or graphitic multi-shell carbon layer (Figure 1c). In some cases, amorphous carbon together with graphitic multi-shell carbon covers the metal nanoparticles (Figure 1d). The white arrows and black arrows label the amorphous carbon and graphitic multi-shell carbon regions, respectively. Due to the chemical inertness of these carbon layers to HCl acid, it is impossible to completely remove the metal nanoparticles only by HCl acid washing. Suitable measures to remove or destroy the carbon layers without much loss of the nanotubes are necessary prior to HCl acid washing. Figure 2 shows the XRD pattern of the as-grown SWNT product. Besides carbonaceous materials, the γ-FeNi alloy phase of the metal nanoparticles formed by alloying of metal Fe and Ni catalysts during the arc-discharge process was identified.

Removal of Amorphous Carbon by CV Oxidation. Figure 3 shows the cyclic voltammograms of the

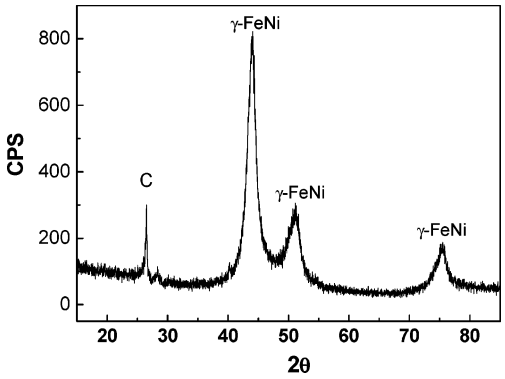

Figure 2. The XRD pattern of the as-grown SWNT product.

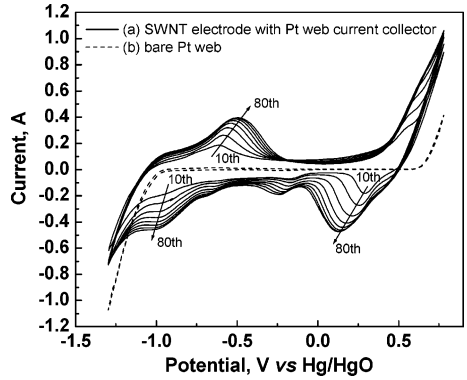

Figure 3. Cyclic volatmmegrams between −1.3 and 0.78 V of (a) the SWNT electrode with Pt web current collector and (b) the bare Pt web.

electrochemical oxidation on the SWNT electrode. The cyclic voltammograms were recorded every 10 cycles. Reduction peaks in the range of −0.96 to −1.0 V and 0.29 to 0.13 V, together with oxidation peaks in the range of −0.61 to −0.49 V, were observed. For compari-

son, a cyclic voltammogram of a bare Pt web electrode with the same weight and surface area as was used in the SWNT electrode is also shown. The bare Pt web electrode did not present any redox peaks even after several tens of cycling, and the increasing current at potentials positive to 0.62 V and negative to −0.96 V was caused by oxygen evolution and hydrogen evolution, respectively. Thus, it can be affirmed that the redox peaks of the SWNT electrode arose from the SWNT sample. The origin of the redox peaks and the reason for their variation along with cycling will be discussed in the next section.

It has been reported that the oxidation of acetylene black happened when the potential was higher than 0.45 V, and the reaction products of carbon electrochemical oxidation in KOH solution were CO_3^{2-} and CO gas.[26] Accordingly, the oxidation corrosion of carbonaceous materials in the SWNT sample occurred upon sweeping the potential positive to 0.45 V in the CV oxidation. Highly disordered carbons are more readily oxidized electrochemically.[26] Based on this point, during the CV oxidation, amorphous carbon with a high disorder degree and hence low stability is preferential for oxidation, then finally realizing the removal of the amorphous carbon from the as-grown SWNT product.

It is well-known that amorphous carbon is composed of sp^3 carbon and sp^2 carbon, and carbon nanotubes are mainly constructed of sp^2 carbon. By analyzing the ratio between sp^2 carbon and sp^3 carbon, it can be clarified whether amorphous carbon in the SWNT product is removed by the CV oxidation treatment. According to the report of Díaz et al.,[30] the XPS analysis method was adopted successfully to characterize the variation of sp^2 carbon and sp^3 carbon in a carbon film during heat treatment. Here, we use XPS method to analyze the content variation of the amorphous carbon in the SWNT sample. Figure 4 shows C1s XPS analysis results of the SWNT samples before and after the CV oxidation treatment for 80 cycles. To identify the C1s XPS results, a curve-fitting procedure was employed. Dots shown in Figure 4 correspond to XPS experimental data, and bold solid lines are fitting curves for the experimental data. The C1s spectra of the as-grown SWNT sample can be fitted with three peaks at 284.3, 285.2, and 288.9 eV. The asymmetric peak at 284.3 eV and the symmetric peak at 285.2 eV can be attributed to sp^2 carbon and sp^3 carbon, respectively.[30,31] The asymmetric parameter of sp^2 carbon was decided by fitting the C1s spectra of a basal plane of highly oriented pyrolytic graphite. The peak at 285.2 eV is mainly from the sp^3 carbon in the amorphous carbon. The sp^2 carbon in both amorphous carbon and nanotube carbon contributes to the peak at 284.3 eV, and the peak at 288.9 eV is from the O=C−O functional group. The O1s spectrum of the as-grown SWNT sample (Figure 4b) shows two components at 530.6 and 531.8 eV, corresponding to C=O and C−O in the O=C−O functional group, respectively. The detection of oxygen-containing functional groups in our arc-derived SWNT sample is in agreement with other

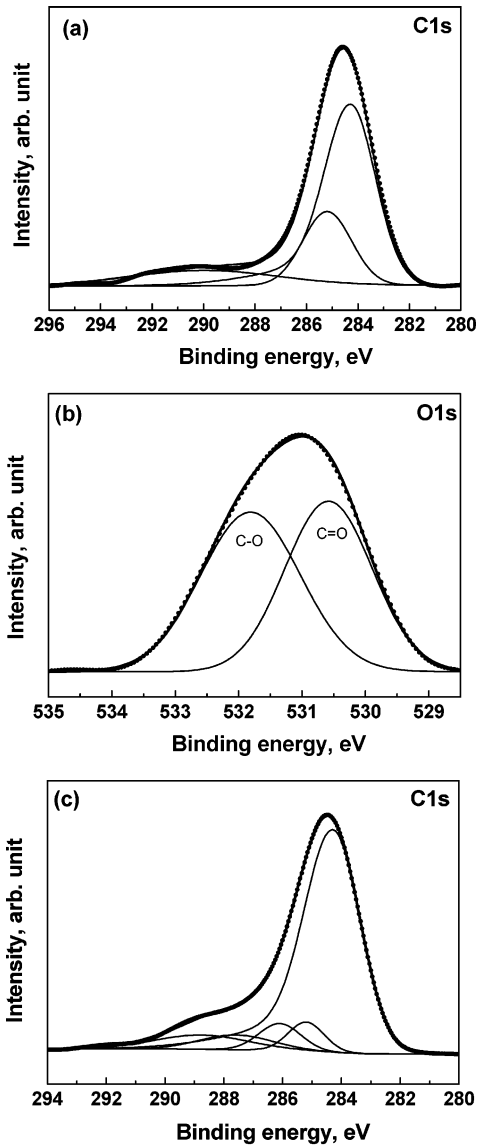

Figure 4. XPS spectra of the SWNT samples. (a) C1s and (b) O1s before the CV oxidation and (c) C1s after the CV oxidation for 80 cycles.

reports.[16,32] After the CV oxidation treatment for 80 cycles, two new peaks appear at 286.1 and 287.6 eV, and they are from C−O and C=O functional groups, respectively. More importantly, by comparing the C1s XPS spectra of the SWNT sample before and after the CV oxidation for 80 cycles, it can be found that the sp^2/sp^3 carbon ratio obviously increases, indicating that the amorphous carbon in the as-grown SWNT sample was removed effectively by the CV oxidation treatment.

Because the amorphous carbon was removed and, consequently, more metal nanoparticles covered by amorphous carbon layer (as shown in Figure 1b) or discontinuous multi-shell carbon (as shown in Figure 1d) were exposed or partially exposed after the CV oxidation treatment, subsequent HCl acid washing will effectively decrease the content of the metal nanoparticles in the SWNT sample, thus attaining the purpose of purification. Figure 5 shows a HRTEM micrograph of the SWNT sample purified by the CV

(30) Díaz, J.; Paolicelli, G.; Ferrer, S.; Comin, F. *Phys. Rev. B* **1996**, *54*, 8064.

(31) Ago, H.; Kugler, T.; Cacialli, F.; Salaneck, W. R.; Shaffer, M. S. P.; Windle, A. H.; Friend, R. H. *J. Phys. Chem. B* **1999**, *103*, 8116.

(32) Lee, Y. S.; Cho, T. H.; Lee, B. K.; Rho, J. S.; An, K. H.; Lee, Y. H. *J. Fluorine Chem.* **2003**, *120*, 99.

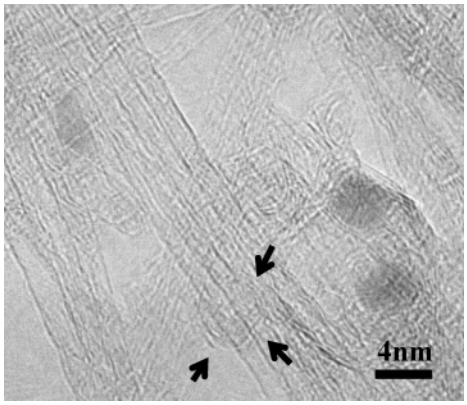

Figure 5. HRTEM micrograph of the purified SWNT sample.

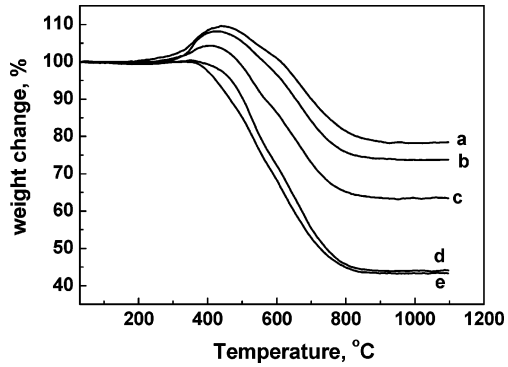

Figure 6. TGA results of (a) the as-grown SWNT product, (b) the SWNT sample only washed with HCl, (c) the SWNT sample after CV oxidation for 40 cycles and HCl washing, (d) the SWNT sample after CV oxidation for 80 cycles and HCl washing, and (e) the SWNT sample after CV oxidation for 120 cycles and HCl washing.

oxidation treatment for 80 cycles and subsequent HCl washing. In comparison with the as-grown SWNT product as shown in Figure 1, amorphous carbon is absent in the purified SWNT sample either on the surface of the nanotubes or on the residual metal nanoparticles. This is consistent with the C1s XPS analysis results. Because graphitic multi-shell carbon layers are less defective and hard corroded, the metal nanoparticles encased in continuous graphitic multi-shell carbon (as shown in Figure 1c) remained after the purification. Therefore, some metal nanoparticles encapsulated in the muti-shell carbon still exist in the purified sample. Furthermore, it is interesting to observe an empty carbon nanocapsule labeled with black arrows in Figure 5, which is supposed to be from a metal nanoparticle with discontinuous muti-shell carbon layers, as shown in Figure 1d. The amorphous carbon region of the carbon layer was opened by CV oxidation, and the partially exposed metal nanoparticles were removed by subsequent acid washing, leaving the empty carbon nanocapsules.

Figure 6 shows the TGA results of the as-grown SWNT sample, and the SWNT sample treated by the CV oxidation for different cycles and subsequent HCl washing. For comparison, the TGA result of the SWNT sample that experienced only HCl washing treatment is also shown. It can be seen that obvious weight gain is present at 500 °C for the as-grown SWNT sample, the HCl washed sample, and the sample after 40-cycle electrochemical oxidation, respectively. The air oxidation of carbon and metals leads to weight decrease and weight increase, respectively. If the content of the metal impurities is relatively high, the weight increase can be predominant and mask the weight loss, resulting in the increase of sample relative weight over 100%. The weight loss of the as-grown SWNT sample is only 21.8 wt % after heating to 1100 °C, much lower than the common values (60−70 wt %) of pristine arc-derived SWNT samples reported,[17,19,33] indicating the higher content of the metal impurities in this selected sample for purification investigation. By assuming all metal impurities were converted into metal oxides, the content of metal in the as-grown SWNT sample can be estimated to be as high as about 60 wt %. The oxidation of high content metal nanoparticles in our selected as-grown SWNT sample is the reason for the weight gain.

The residue after the TGA experiment of the SWNT sample only washed with HCl is as high as 73.6 wt %, a little lower than the pristine sample, indicating the limitation of simple HCl washing because most metal nanoparticles were encased in amorphous carbon or graphitic multi-shell carbon. The CV oxidation for 40 cycles is not enough, because a weight gain peak at 500 °C is still present in the TGA curve and the residue weight is as high as 63.5 wt %, as shown in Figure 6, curve c. With respect to the SWNT sample purified by the CV oxidation for 80 cycles and HCl washing, no weight gain peak at 500 °C is present, and the percent of the residue decreases to 43.8 wt %, illustrating an evident decrease of the metal content after the purification procedure. In combination with the results of the HRTEM observations and C1s XPS analysis, it can be concluded that the described purification method involving the electrochemical oxidation is effective. However, a certain content of metal nanoparticles still remains in the purified SWNT sample, as is shown in the HRTEM image (Figure 5) and is illustrated in the TGA analysis. To further remove metal impurities, an attempt to expose more metal nanparticles by increasing the cycle number of the CV oxidation was tried. However, no significant improvement was obtained. For instance, even after the SWNT sample was treated by the CV oxidation for 120 cycles, there was no evident improvement in the TGA result as shown in Figure 6, curve e. This result indicates that graphitic multi-shell carbon with less defects and hence higher oxidation resistance can hardly be destroyed by the CV oxidation without much loss of the nanotubes.

The oxidation resistance of graphitic multi-shell carbon layers on the survival metal nanoparticles is comparable to the nanotubes. The multi-shell carbon layers are hard removed without much loss of the nanotubes. In this regard, the mechanical purification method[32] or the microwave-assisted purification[34,35] method can be applied as the following steps to further remove the residual metal nanoparticles. On the other hand, if as-grown SWNT products with a higher content of nanotubes and less content of metal nanoparticles

(33) Thiên-Nga, L.; Hernadi, K.; Ljubović, E.; Garaj, S.; ForrÓ, L. *Nano Lett*. **2002**, *2*, 1349.
(34) Harutyunyan, A. R.; Pradhan, B. K.; Chang, J.; Chen, G.; Eklund, P. C. *J. Phys. Chem. B* **2002**, *106*, 8671.
(35) Martínez, M. T.; Callejas, M. A.; Benito, A. M.; Master, W. K.; Cochet, M.; Andrés, J. M.; Schreiber, J.; Chauvet, O.; Fierro J. L. G. *Chem. Commun.* **2002**, 1000.

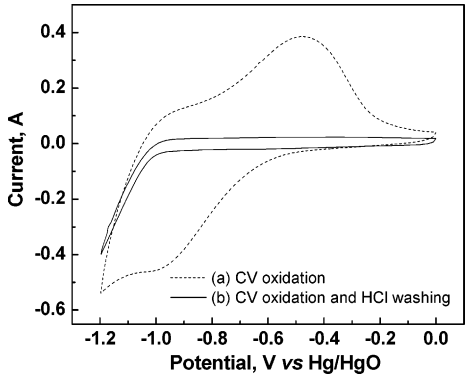

Figure 7. Cyclic voltammograms between −1.2 and 0 V of the SWNT electrode that experienced (a) the CV oxidation for 80 cycles, (b) the CV oxidation for 80 cycles and subsequent HCl washing treatment.

encased in continuous graphitic multi-shell carbon are purified by this process, better results can be expected.

Benchmark for the Removal Extent of Amorphous Carbon. It is noteworthy that the potential and current of all reduction and oxidation peaks are dependent on the cycle number. As is evidently shown in Figure 3, the current of all peaks increases with cycle number prior to the 80th cycle. The increase rate of peak current gradually reduces, and finally the peak current remains almost unchanged after 80 cycles. Meanwhile, positive potential shift and negative potential shift were observed for the observed oxidation peaks and reduction peaks, respectively.

Consistent with the 80th cycle between −1.3 and 0.78 V, for the SWNT electrode that experienced CV oxidation for 80 cycles, an oxidation peak at −0.49 V and a reduction peak at −1.0 V are also present during voltammetric cycling between −1.2 and 0 V as shown in Figure 7. These two redox peaks are reproducible within several tens of cycles between −1.2 and 0 V. We found that the oxidation and reduction peaks disappeared simultaneously if the CV oxidized SWNT sample was washed in HCl solution to remove the exposed metal nanoparticles. The absence of the redox response after HCl washing indicates that the redox peaks are associated with the electrochemical oxidation and reduction of metal impurities. It is reasonable to consider that the comparison of the chemical states of the metal impurities at −1.2 V with that at 0 V is useful to clarify both the oxidation peak and the reduction peak. Accordingly, two SWNT electrodes oxidized for 80 cycles were cycled between −1.2 and 0 V, and stopped at 0 and −1.2 V, respectively. The chemical states of the metal impurities in these two SWNT electrodes were compared using XPS analysis. Figure 8a and b shows Fe $2p^{3/2}$ and Ni $2p^{3/2}$ XPS spectra, respectively.

The peak at 706.9 eV in Figure 8a can be attributed to metallic Fe, and the other two peaks above 710 eV can be attributed to Fe oxides with different chemical valences. The peaks at 852.0 and 856.2 eV in Figure 8b are from metallic Ni and Ni(II) oxide, respectively. Note that the binding energy of the Fe oxides in the SWNT sample stopped at 0 V is higher than that in the sample stopped at −1.2 V, and the peak intensity of metallic Fe (Fe $2p^{3/2}$ 706.9 eV) in the SWNT sample stopped at 0 V is lower than that in the sample stopped at −1.2 V. The former indicates partial transformation between Fe-

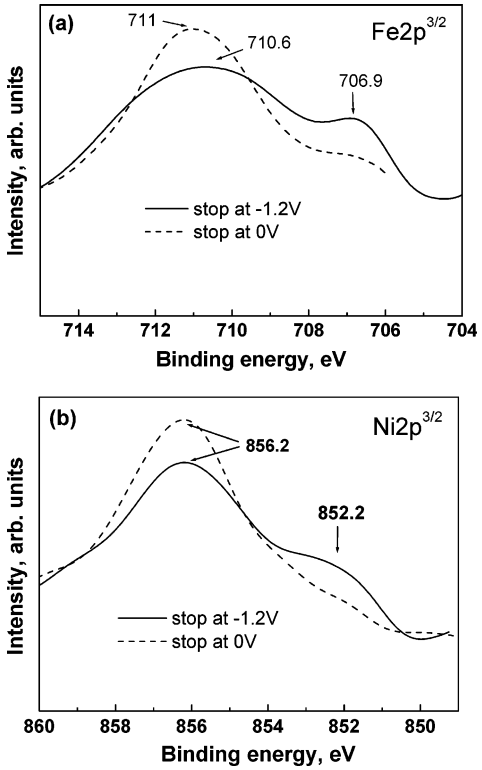

Figure 8. Fe $2p^{3/2}$ and Ni $2p^{3/2}$ XPS analysis of the CV oxidized SWNT sample (after 80 cycles) stopped at 0 and −1.2 V.

(II) oxide and Fe(III) oxide, and the latter indicates the content change of the metallic Fe as a result of the transformation between metallic Fe and Fe(II) oxide. Although no position change of the Ni XPS peak was observed, by analogy with the Fe XPS results, the content change of metallic Ni and Ni(II) oxide as observed in Figure 7b indicates the transformation between metallic Ni and Ni(II) oxide. Therefore, it can be concluded that the reduction peaks in the range of −0.96 to −1.0 V and the oxidation peaks in the range of −0.61 to −0.49 V present in CV oxidation are attributed to the electrochemical redox transformation between metallic Fe and Fe(II) oxide, Fe(II) oxide and Fe(III) oxide, as well as Ni and Ni(II) oxide. The related electrochemical redox reactions are listed below.

$$Fe(OH)_2 + 2e^- \leftrightarrow Fe + 2OH^- \qquad \varphi^0 = -0.86\ V$$

$$Fe(OH)_3 + e^- \leftrightarrow Fe(OH)_2 + OH^- \qquad \varphi^0 = -0.56\ V$$

$$Ni(OH)_2 + 2e^- \leftrightarrow Ni + 2OH^- \qquad \varphi^0 = -0.70\ V$$

Because of overpotential in the electrochemical redox reactions under the potential scan condition, there are differences between these standard potentials and the redox peak potentials.

NiOOH formation and its reduction on Ni electrode in the potential range of 0.36−0.28 V (vs Hg/HgO) were well investigated in some literature.[36−42] By the same

(36) Kibria, M. F.; Mridha, M. S. *Int. J. Hydrogen Energy* **1996**, *21*, 179.
(37) Dmochowska, M.; Czerwiński, A. *J. Solid State Electrochem.* **1998**, *2*, 16.
(38) Bode, H.; Dehmelt, K.; Witte, J. *Electrochim. Acta* **1966**, *11*, 1079.

reaction mechanism, the metallic Ni could be oxidized into NiOOH during the positive scan of the CV oxidation treatment. The observed reduction peaks in the potential range of 0.29−0.13 V are believed to be caused by the electrochemical reduction of NiOOH into $Ni(OH)_2$.

During CV oxidation cycling, more and more metal nanoparticles could be exposed to the KOH solution due to the incremental removal or damage of the amorphous carbon coating by the oxidation, and then more exposed metal nanoparticles could participate in the electrochemical oxidation and reduction reactions. As a result, the intensity of all of the redox peaks increased with the CV oxidation. Once the removal of the amorphous carbon by the oxidation was completed, the amount of the exposed metal nanoparticles would not increase, and thus the intensity of the redox peaks remained almost unchanged. In other words, the intensity variation of the redox peaks can be used to indicate the removal extent of the amorphous carbon. When the intensity of the redox peaks present in the CV oxidation curves remains unchanged, at the 80th cycle of our selected SWNT sample, it can be judged that the amorphous carbon is completely removed. This is the reason why no significant improvement on purification was obtained after the CV oxidation for more than 80 cycles (such as 120 cycles, see Figure 6). To avoid much loss of carbon nanotubes, the oxidation cycle number should be suitable because the nanotubes will be destroyed in excessive CV oxidation treatment. Because the intensity variation of the redox peaks indicates the removal extent of the amorphous carbon, the suitable cycle number can be determined in real time by observing the variation of the redox peaks during the CV oxidation. The CV oxidation should be stopped at the cycle during which the redox peaks remain almost unchanged.

With voltammetric cycling, the oxidation peak positively shifted from −0.61 to −0.49 V, and the two reduction peaks negatively shifted from −0.96 to −1.0 V and from 0.29 to 0.13 V, respectively. We thought that some unreducible metal oxides could be formed more and more on the surface of the γ-FeNi impurity nanoparticles with voltammetric cycling. Gradually, incremental unreducible metal oxides could hinder further electrochemical redox reactions of Fe and Ni impurities and hence cause increasing overpotentials, which led to the continuous positive and negative shift for the oxidation peaks and reduction peaks, respectively. For instance, it has been confirmed in some literature that gradually incremental unreducible β-$Ni(OH)_2$ was formed on Ni electrode during a CV experiment in a wide enough potential scan range.[36,37] We believe that unreducible β-$Ni(OH)_2$ could also be formed on the γ-FeNi impurity nanoparticles, thus leading to the shift of the redox peaks.

Conclusions

Amorphous carbon in the as-grown SWNT product was effectively eliminated during the CV oxidation treatment, and then the metal impurity nanoparticles coated by amorphous carbon or discontinuous graphitic multi-shell carbon were exposed and removed by subsequent HCl washing. These results indicate that the CV oxidation can be applied as an alternative oxidative treatment for the purification of SWNT samples besides gas-phase oxidation and wet oxidation. This new oxidation treatment can be scaled up if one uses a high power potentiostat. Furthermore, the redox peaks from the electrochemical redox reactions of Fe and Ni impurities can be considered as a benchmark for judging the removal extent of the amorphous carbon. Most amorphous carbon is eliminated at the cycle during which the redox peaks remain almost unchanged. By this point, the optimal cycle number can be determined during the CV oxidation treatment, hence avoiding heavy loss or damage of the nanotubes. Therefore, superior to the gas-phase oxidation and wet oxidation, the optimal time and degree of the electrochemical oxidation for the SWNT purification can be determined in real time.

It was also confirmed that XPS analysis was a useful and simple method to evaluate the content variation of amorphous carbon in SWNT samples by analyzing the sp^3/sp^2 carbon ratio. The result is consistent with the HRTEM observations.

Acknowledgment. This work was supported by the National Science Foundation of China (Grants 50025204, 50472084 and 50328204), the Special Funds for Major State Basic Research Projects (Grant G2000026403), the China Postdoctoral Science Foundation, and the K. C. Wong Education Foundation, Hong Kong.

CM035263H

(39) Schrebler Guzmán, R. S.; Vilche, J. R.; Arvia, A. J. *J. Electrochem. Soc.* **1978**, *125*, 1578.
(40) Hahn, F.; Beden, B.; Croissant, M. J.; Lamy, C. *Electrochim. Acta* **1986**, *31*, 335.
(41) Singh, D. *J. Electrochem. Soc.* **1998**, *145*, 116.
(42) Czerwiński, A.; Dmochowska, M.; Grdeń, M.; Kopczyk, M.; Wójcik, G.; Młynarek, G.; Kołata, J.; Skowroński, J. M. *J. Power Sources* **1999**, *77*, 28.